

# Determination of Radioactivity Levels and Radiation Hazards in Coastal Sediment Samples of Chennai Coast, Tamilnadu, India using Gamma Ray Spectrometry with Statistical Approach

M. Tholkappian<sup>1</sup>, A. Chandrasekaran<sup>2</sup>, Durai Ganesh<sup>3</sup>, J.Chandramohan<sup>4</sup>, N. Harikrishnan<sup>3</sup> and R. Ravisankar<sup>3,\*</sup>

<sup>1</sup>Department of Physics, Sri Vari College of Education, Then Arasampattu, Tiruvannamalai - 606611, Tamilnadu, India.

<sup>2</sup>Department of Physics, SSN College of Engineering, Kalavakkam, Chennai, Tamilnadu - 603110, India

<sup>3</sup>Post Graduate and Research Department of Physics, Government Arts College, Tiruvannamalai- 606603, Tamilnadu, India

<sup>4</sup>Department of Physics, Sun Arts and Science College, Tiruvannamalai—606755, Tamilnadu, India

Received: 3 Jul. 2018, Revised: 23 Aug. 2018; Accepted: 28 Aug. 2018

Published online: 1 Sep. 2018.

**Abstract:** Radioactivity of the sediment environment is one of the main sources of exposure to humans. The concentration of radionuclides in marine sediments can provide very useful information on the source, transport mechanisms and environmental fate of radionuclides. In this work, the coastal sediment samples are addressed to find out any radiation hazard associated with the sediments. The sediment samples were collected from Pulicatlake to Vadanemeli of Chennai coast, Tamilnadu using Peterson grab sampler from 10 m water depths parallel to the seashore line. Gamma radiation measurements were performed using NaI(Tl) detector PC multichannel Spectrometer. The specific activity concentration of radionuclides Uranium (<sup>238</sup>U), Thorium (<sup>232</sup>Th) and Potassium (<sup>40</sup>K) were investigated and mean specific activity values <sup>238</sup>U (10.14 Bq kg<sup>-1</sup>), <sup>232</sup>Th (35.02 Bq kg<sup>-1</sup>) and <sup>40</sup>K (425.8 Bq kg<sup>-1</sup>) were tabulated. The average activity of <sup>232</sup>Th is slightly greater than the world average value. The assessment of radiation hazard associated with the sediment is computed using the radiation indices like Radium Equivalent Activity (Ra<sub>eq</sub>), Absorbed Gamma Dose Rates in air (D<sub>R</sub>), the Annual Effective Dose Equivalent (AEDE), Annual Gonadal Dose Equivalent (AGDE), Representative level index (RLI), Activity Utilization Index (AUI), Internal Hazard Index (H<sub>in</sub>), External Hazard Index (H<sub>ext</sub>), and Excess Lifetime Cancer (ELCR) is compared with internationally recommended values and safety limits. The multivariate statistical analysis has been carried out for the radiological data and it is used to find out any existing relationship between radioactive variables. The results of these investigations are presented and discussed in this paper.

**Keywords:** Natural Radioactivity, Sediment, Radiation Hazard, Statistical Analysis.

## 1 Introduction

Natural radioactivity is a source of continuous exposure to human beings. Human beings are constantly exposed to natural sources of ionizing radiations in nature. Natural radioactivity and the associated external exposure due to gamma radiation depend primarily on the geological and geographical conditions in each region of the world. The assessment of gamma radiation dose from natural sources is of particular importance because natural radiation is the largest contributor to the external dose of the world

population [1]. These dose rates vary from place to place depending upon the concentration of natural radionuclides like <sup>232</sup>U, <sup>232</sup>Th and their progeny and the activity of singly occurring radionuclide <sup>40</sup>K present in soil, sediment and rocks. The activity of natural radionuclides in soil and sediment depends mainly on the types of rocks from which they originate. These radionuclides pose exposure risks externally due to their gamma-ray emissions and internally due to radon and its progeny that emit alpha particles [2]. The measurement for the effects of radioactive elements on the environment and human health has increased in the last

\*Corresponding author e-mail:ravisankarphysics@gmail.com

few decades. Obtaining activity concentrations of natural radionuclides are useful not only for the above-mentioned reasons, but also for radiation risk assessment.

The radionuclide contents in coastal marine sediments are mainly derived from terrestrial areas. The estimation of radiation hazard parameters in marine sediments can reflect the health hazards due to natural radiation from nearby terrestrial areas as well as the hazards to people who handle these sediments.

The objective of this paper is to define baseline levels of radioactivity for Chennai coast which can be characterized by naturally radioactivity in some areas because of the heavy mineral and radioactivity bearing minerals which may be present in this area. Moreover, baseline environmental geochemical data are necessary to inform policy makers and provide a sound basis for legislation, addressing in particular public concerns regarding environmental radioactivity.

This evaluation aims to:

1. Establish a reference level of activity concentrations of primordial radionuclides.
2. Correlate the radioactivity concentration with the radiation parameters.
3. Identify areas which may be radiologically hazardous for the public.
4. To employ statistical methods to find existing relationship between activity concentration and radiation indices.

## 2 Materials and Methods

### 2.1 Sample Collections

Sediment samples were collected by a Peterson grab sampler along the Bay of Bengal coastline, from Pulicat lake to Vadanemmeli of Chennai coast of East Coast of Tamilnadu, India during pre-monsoon condition. The sample selection is chosen in pre-monsoon condition, when sediment texture and ecological conditions can be clearly observed, erosional activities are predominant and sediments were not transported from the river and estuary towards the beach and marine. Figure 1 shows the sampling location of the study area. The sampling locations were selected based on the prevailing stresses and included areas near the urban and domestic effluent discharge point.

The grab sampler collects the samples at 10 m below the seabed in all sampling points. Around 25 cm thick subsurface samples from the seabed were collected by the grab. From this, 10 cm thick sediment layer was sampled from the middle of the grab to avoid metal contamination by the jaws of the grab. Table 1 shows the geographic coordinates (latitudes and longitudes) of the various sampling locations. Global positioning system was utilized to locate position of sampling points. The distance between two stations such as Pulicat Lake and Konankuppam was of 3 nautical miles. This distance is kept constant among all the 22 sampling stations. Coastal craft was utilized for

collecting samples at each station. The sample collection personnel approach the beach opposite to the designated sampling station by road and hire boat from artisanal fisherman to approach the sampling point located within 60 min of sailing. This approach was adopted for all the 22 sampling locations to collect samples.

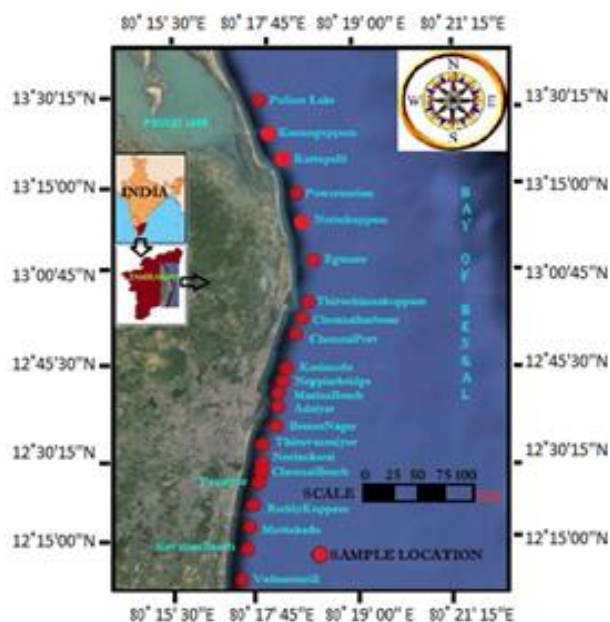


Fig. 1. Location map of the study area.

### 2.2 Sample Preparation

The collected samples were immediately transferred to polyethene bags to avoid the sediment sample's contact with the metallic dredge, and the top sediment layer was scooped with an acid washed plastic spatula. Samples were stored in plastic bags and kept in refrigeration at 4°C until analysis. Then, the samples were air dried at 105°C to a constant weight and sieved through 250 $\mu$  mesh. The homogenized sample was placed in a 250g airtight PVC container. The inner lid was placed and closed tightly with outer cap. Each sediment sample container was left for at least 5 weeks to reach secular equilibrium between  $^{238}\text{U}$  ( $^{226}\text{Ra}$ ) and  $^{232}\text{Th}$  ( $^{228}\text{Ra}$ ) and their progenies.

### 2.3 Measurement of the Samples by Gamma Ray Spectrometry

Sediment samples were subjected to gamma spectral analysis with a counting time of 20,000 s. A 3 inch  $\times$  3 inch NaI (TI) detector was employed with adequate lead shielding which reduced the background by a factor of about 95%. The concentrations of various radionuclides of interest were determined in Bq kg $^{-1}$  using the count spectra. To find out the radioactivity content in sediment samples, the systems have to be efficiency calibrated for various energies of interest in the selected sample geometry. The natural radioactive elements  $^{40}\text{K}$ , uranium, and thorium, the

gamma energies selected are 1460 keV for  $^{40}\text{K}$ , 1763 keV

**Table 1. Geographic coordinates (latitudes and longitudes) of the various sampling locations**

S. No.	Sample ID	Latitude(N)	Longitude(E)	Location
1	CPL	13°34'3.82"N	80°18'0.75"E	Pulicat Lake
2	CPK	13°25'31.42"N	80°21'26.12"E	Pulicat (Koonangkuppam)
3	CKP	13°19'27.33"N	80°22'51.77"E	Kattupalli
4	CPS	13°15'35.37"N	80°22'21.94"E	Power Station
5	CNK	13°14'10.50"N	80°21'53.23"E	Nettukuppam
6	CEE	13°12'41.88"N	80°21'18.71"E	Ennore
7	CTK	13° 9'36.02"N	80°20'32.34"E	Tiruchinnakuppam
8	CCH	13° 8'20.61"N	80°20'8.02"E	Chennai Harbor (Nagooranthottam)
9	CPT	13° 6'5.45"N	80°19'44.78"E	Chennai Port (KasimeduFishing Harbour)
10	CKU	13° 7'14.61"N	80°19'44.04"E	Kasimedu-Tondiarpet
11	CNB	13° 4'17.77"N	80°19'34.47"E	Neppiar Bridge
12	CMB	13° 2'34.23"N	80°18'20.02"E	Marina Beach
13	CBB	13° 0'54.40"N	80°18'21.48"E	Broken Beach (Adaiyaramaram)
14	CBN	13° 0'8.21"N	80°18'17.37"E	Besent Nagar
15	CTR	12°59'8.39"N	80°18'0.98"E	Thiruvanmiyur
16	CNI	12°57'2.18"N	80°17'29.61"E	Neelankarai
17	CCG	12°55'3.90"N	80°17'16.44"E	Chennai Golden Beach
18	CPR	12°53'2.32"N	80°17'4.18"E	Panaiyur
19	CKI	12°50'12.66"N	80°16'34.01"E	Kanathursunami, (Reddykuppam)
20	CMK	12°48'36.74"N	80°16'40.72"E	Muttukaadu (Karikkattukuppam)
21	CKB	12°47'24.36"N	80°16'48.33"E	Kovalam Beach
22	CVM	12°44'59.05"N	80°16'39.20"E	Vadanemmeli, (Puthiyakalpakkam)

( $^{214}\text{Bi}$ ) for uranium, and 2614 keV (from daughter product ( $^{208}\text{Tl}$ ) for thorium. The detection limit of NaI(Tl) detector system for  $^{40}\text{K}$ ,  $^{238}\text{U}$ , and  $^{232}\text{Th}$  is 8.50, 2.21, and 2.11 Bq/kg respectively for a counting time of 20,000s. [3-5].

### 3 Results and Discussion

#### 3.1 Radionuclides ( $^{238}\text{U}$ , $^{232}\text{Th}$ and $^{40}\text{K}$ ) Contents

The results of analysis of activity concentration of  $^{238}\text{U}$ ,  $^{232}\text{Th}$  and  $^{40}\text{K}$  radionuclides in sediment samples for different locations of the study area are presented in Table 2. The range and average values (in brackets) of the activities for  $^{238}\text{U}$ ,  $^{232}\text{Th}$  and  $^{40}\text{K}$  are  $\leq 2.21 - 31.03$  (10.14),  $\leq 2.11 - 168.4$  (35.02) and  $330.9 - 540$  (425.8) Bq  $\text{kg}^{-1}$  respectively. Measured activities of the radionuclides differed widely, as activity levels in the marine environment depend on their physical, chemical and geochemical properties and the environment [6]. In all samples, activity concentrations were in the order  $^{40}\text{K} > ^{232}\text{Th} > ^{238}\text{U}$ .

$^{40}\text{K}$  dominates over the other isotopes because it is the most abundant in continental rocks and it is elevated in many light minerals [7].  $^{232}\text{Th}$  was higher than  $^{238}\text{U}$  in all samples. This could be related to their difference in chemical speciation and solubility in a natural environment.  $^{232}\text{Th}$  is insoluble and also preferentially accumulated on the particular phases relative to  $^{238}\text{U}$  [8]. From the results it is clear that the mean activity of  $^{238}\text{U}$  and  $^{232}\text{Th}$  are lower while  $^{40}\text{K}$  is higher when compared with worldwide average value (Table.3). Fig. 2 shows the variation of activity concentration at different sampling locations.

#### 3.2 Evaluation of Radiological Hazard Effects

In order to determine the radiation hazard due to the natural radioactivity associated with the sediments, different radiological parameters are estimated and their values are compared with internationally approved values and recommended safety limits. Table 2 lists the computed

radiological parameters of the sediment in the study area.

### 3.2.1 Radium Equivalent Activity ( $Ra_{eq}$ )

The radium equivalent activity is an index that represents the specific activities of  $^{232}\text{U}$ ,  $^{232}\text{Th}$  and  $^{40}\text{K}$  by a single quantity which takes into account the radiation hazards associated with them. To compare the radiological effects of the coastal sediment samples, which contain  $^{238}\text{U}$ ,  $^{232}\text{Th}$  and  $^{40}\text{K}$ , a common index is required to obtain the sum of activities. This index is usually called the radium equivalent activity ( $Ra_{eq}$ ) as given in the following expression [9-11].

$$Ra_{eq} = A_U + 1.43A_{Th} + 0.077A_K \quad \text{----- (1)}$$

Where  $A_U$ ,  $A_{Th}$  and  $A_K$  are the specific activities of  $^{238}\text{U}$ ,  $^{232}\text{Th}$  and  $^{40}\text{K}$  ( $\text{Bq kg}^{-1}$ ) respectively. It has been assumed here that  $370 \text{ Bq kg}^{-1}$  of  $^{238}\text{U}$  or  $259 \text{ Bq kg}^{-1}$  of  $^{232}\text{Th}$  or  $4810 \text{ Bq kg}^{-1}$  of  $^{40}\text{K}$  produce the same gamma dose rate.  $Ra_{eq}$  is related to the external  $\gamma$ -dose and internal dose due to radon and its daughters. The maximum value of  $Ra_{eq}$  in sediment samples is required to be less than the limit value of  $370 \text{ Bq kg}^{-1}$  recommended by the Organization for Economic Cooperation and Development for safe use.

The Radium Equivalent Activity ( $Ra_{eq}$ ) in these sediment samples ranges from  $36.96 \text{ Bq kg}^{-1}$  (CNK) to  $305.49 \text{ Bq kg}^{-1}$  (CVM) with a mean value of  $93.0 \text{ Bq kg}^{-1}$  (Table 2) which is less than the recommended maximum value of  $370 \text{ Bq kg}^{-1}$ . It indicates that no radiological hazards are associated with the sediments. Fig. 2 shows variation of Radium equivalent activity ( $Ra_{eq}$ ) in different locations.

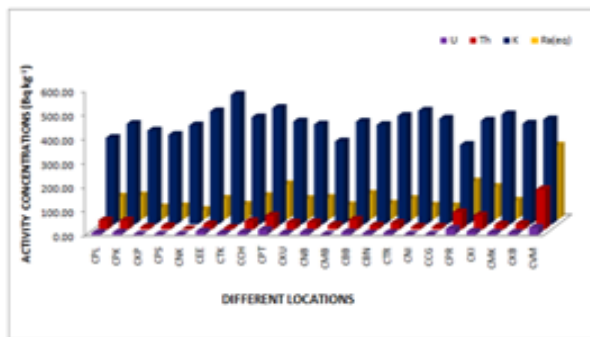


**Fig. 2.** Location Vs Activity Concentration and Radium Equivalent Activity ( $\text{Bq kg}^{-1}$ )

### 3.2.2 Absorbed Gamma Dose Rate ( $D_R$ )

Absorbed gamma dose rate is the amount of energy from ionizing radiations. The absorbed per unit mass per unit time of matter, expressed in Grays. The absorbed dose rate is important in radiation risk analysis since it measures the amount of radiation deposited per unit time. The contribution of natural radionuclides to the absorbed dose rate in air ( $D_R$ ) depends on the natural

specific activity concentration of  $^{238}\text{U}$ ,  $^{232}\text{Th}$  and  $^{40}\text{K}$ .

The outdoor air-absorbed dose rates due to terrestrial gamma rays at 1 m above the ground were calculated from  $^{238}\text{U}$ ,  $^{232}\text{Th}$  and  $^{40}\text{K}$  concentration values in sediments assuming that the other radionuclide's, such as  $^{137}\text{Cs}$ ,  $^{90}\text{Sr}$  and  $^{235}\text{U}$  decay series can be neglected as they contribute very little to the total dose from environmental background [11-13]. The absorbed dose rate is calculated from the equation given below.

$$D_R (\text{nGyh}^{-1}) = 0.462A_U + 0.604A_{Th} + 0.042A_K \quad \text{----- (2)}$$

The range of absorbed dose rate in air due to natural radionuclides (Table 2) in the studied area is  $37.32$  (CNK) –  $248.75$  (CVM)  $\text{nGyh}^{-1}$  with the mean of  $81.91 \text{ nGyh}^{-1}$ . From Table 2, it is clear that mean value of absorbed dose rate in the studied area is nearly equal to the world average Absorbed Gamma Dose Rate of  $84 \text{ nGyh}^{-1}$  [1]. All locations except Pulicat (CPK), Chennaiharbor (CCH), Chennai Port (CPT), Broken beach (CBB), Panaiyur (CPR), Kanathursunami Area (CKI) and vadanemmeli (CVM) noticed higher value than the world average value. The high values could be explained as due to the presence of black sands, which are enriched in the mineral monazite containing a significant amount of  $^{232}\text{Th}$ . This may have enhanced the activity concentrations which reflect the higher value of the absorbed dose rate. Fig. 3 shows the variation of absorbed gamma dose rate in different locations.

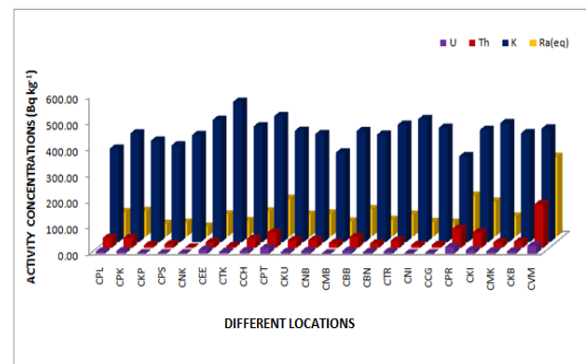


**Fig.3.** Locations Vs Absorbed Gamma Dose rate ( $\text{nGyh}^{-1}$ )

### 3.2.3 Annual Effective Dose Equivalent (AEDE)

In order to estimate the annual effective dose rates, one has to take into account the conversion coefficient from the absorbed dose in air to the effective dose received by adults ( $0.7 \text{ SvGy}^{-1}$ ) and the outdoor occupancy factor (0.2) which implies that people spend 20% of the time outdoors, on the average, around the world proposed by UNSCEAR (2000)[1]. As the determination of AEDE of each site sample is very important, Annual effective dose for radon concentrations (in  $\text{Bq/m}^3$ ) was calculated according to the

equation [1].

**Table 2: Radiological parameters in Coastal sediment samples of East Coast line of Stud Area**

Sample ID	Activity Concentration (Bqkg <sup>-1</sup> )			Ra <sub>(eq)</sub> (Bqkg <sup>-1</sup> )	Gamma Dose Rate (D <sub>R</sub> ) (nGyh <sup>-1</sup> )	Annual Effective dose rate (mSvy <sup>-1</sup> )	Annual Gonadal Dose equivalent	Gamma Representative level index (I <sub>γr</sub> )	Activity Utilization Index (AUI)	H <sub>int</sub>	H <sub>ext</sub>	ELCR X 10 <sup>-3</sup>
	<sup>238</sup> U	<sup>232</sup> Th	<sup>40</sup> K									
CPL	9.3	39.41	360.26	93.4	80.73	0.099	0.307	0.696	0.592	0.277	0.252	0.348
CPK	10.5	38.67	418.46	98.02	85.67	0.105	0.325	0.736	0.599	0.293	0.265	0.369
CKP	2.21	10.98	390.51	47.98	45.35	0.056	0.175	0.385	0.186	0.136	0.13	0.195
CPS	2.21	14.96	372.54	52.29	48.29	0.059	0.186	0.413	0.232	0.147	0.141	0.208
CNK	2.21	2.11	412.09	36.96	37.32	0.046	0.145	0.311	0.08	0.106	0.1	0.161
CEE	15.35	22.68	470.34	84	76.7	0.094	0.29	0.643	0.455	0.268	0.227	0.33
CTK	7.07	7.16	540.02	58.89	57.58	0.071	0.221	0.479	0.197	0.178	0.159	0.248
CCH	10.04	35.7	445.85	95.42	84.17	0.104	0.32	0.721	0.561	0.285	0.258	0.362
CPT	22.24	59.14	485.12	144.16	124.32	0.153	0.468	1.063	0.96	0.449	0.389	0.535
CKU	7.09	30.39	428.69	83.56	74.25	0.091	0.284	0.637	0.468	0.245	0.226	0.32
CNB	11.1	30.94	416.12	87.39	77.54	0.095	0.294	0.661	0.511	0.266	0.236	0.334
CMB	2.21	19.66	345.1	56.9	51.27	0.063	0.197	0.441	0.287	0.16	0.154	0.221
CBB	12.04	41.98	427.33	104.98	91.44	0.112	0.347	0.785	0.654	0.316	0.283	0.394
CBN	6.48	17.72	413.87	63.69	58.56	0.072	0.224	0.496	0.308	0.189	0.172	0.252
CTR	8.64	27.84	451.55	83.22	74.7	0.092	0.285	0.637	0.454	0.248	0.225	0.322
CNI	2.21	11.54	473.13	55.14	52.58	0.065	0.204	0.446	0.199	0.155	0.149	0.226
CCG	2.21	11.54	439.77	52.57	49.91	0.061	0.193	0.423	0.197	0.148	0.142	0.215
CPR	25.98	73.41	330.91	156.44	131.13	0.161	0.491	1.128	1.154	0.493	0.422	0.564
CKI	14.13	60.15	431.85	133.4	113.71	0.14	0.431	0.984	0.893	0.398	0.36	0.49
CMK	9.56	21.74	458.54	75.96	69.39	0.085	0.264	0.587	0.389	0.231	0.205	0.299
CKB	9.29	24.23	419.1	76.21	68.73	0.085	0.262	0.584	0.413	0.231	0.206	0.296
CVM	31.03	168.4	436.99	305.49	248.75	0.306	0.937	2.182	2.357	0.909	0.825	1.071
AVE	10.14	35.02	425.8	93	81.91	0.101	0.311	0.702	0.552	0.279	0.251	0.353
MAX	31.03	168.4	540	305.49	248.75	0.306	0.937	2.182	2.357	0.909	0.825	1.071
MIN	2.21	2.11	330.9	36.96	37.32	0.046	0.145	0.311	0.08	0.106	0.1	0.161

$$AEDE = D_R (nGyh^{-1}) \times 8760 h \times 0.2 \times 0.7 SvGy^{-1} \times 10^{-6}$$

$$AEDE (mSv y^{-1}) = D_R \times 0.00123 \quad \text{--- (3)}$$

The annual effective dose equivalent (Table 2) in the study area ranged between 0.046 (CNK) and 0.306 (CVM) with a mean value of 0.101 mSv y<sup>-1</sup>. The International Commission on Radiological Protection (ICRP) has recommended the annual effective dose equivalent limit of 1 mSvy<sup>-1</sup> for the individual members of the public and 20 mSvy<sup>-1</sup> for the radiation workers [14]. In areas with the normal background radiation, the average annual external effective dose from terrestrial radionuclides is 0.46 mSvy<sup>-1</sup>[15]. Therefore, the obtained mean value from this study area (0.097 mSv y<sup>-1</sup>) is well lower than the world average value. This indicates that the sediment samples

satisfy the criteria from the radiation safety point of view. Fig. 4 shows the variation of Annual Effective Dose Equivalent in different locations.

### 3.2.4 Annual Gonadal Dose Equivalent (AGDE)

The gonads, the activity bone marrow and the bone surface cells are considered as organs of interest because they are the most sensitive parts of the human body to radiation [2]. An increase in annual gonadal Dose Equivalent (AGDE) has been known to affect the bone marrow, causing destruction of the red blood cells that are then replaced by white blood cells. This situation results in a blood cancer called leukemia which is fatal. It is a measure of the genetic significance of the yearly dose equivalent received by the population's reproductive organs (gonads). Therefore, the

Annual Gonadal Dose Equivalent (AGDE) due to the specific activities of <sup>238</sup>U, <sup>232</sup>Th and <sup>40</sup>K was calculated using the following formula [16, 17].

$$AGDE (\mu\text{Sv}^{-1}) = 3.09A_U + 4.18A_{Th} + 0.314A_K \text{ ----- (4)}$$

The AGDE values are presented in Table 2. The Annual Gonadal DoseEquivalent obtained ranged between 0.145 (CNK) and 0.937 (CVM) with a mean value of 0.311 $\mu\text{Sv y}^{-1}$ . As can be seen, the average values do not, in general, exceed the permissible recommended limits, indicating that the hazardous effects of these radiations are negligible. Fig. 4 shows variation of annual gonadal dose equivalent (AGDE) in different locations.

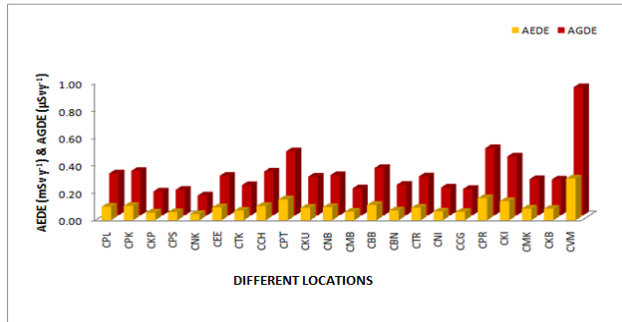


**Fig. 4.** Locations Vs Annual Effective Dose Rate (mSv<sup>-1</sup>) & Annual Gonadal Dose Equivalent (mSv<sup>-1</sup>).

### 3.2.5 Gamma Representative Level Index (I<sub>γr</sub>)

The representative level index (I<sub>γr</sub>) of the sediment may be used to estimate the level of gamma radiation hazard associated with natural gamma emitters in the sediments. Since, gamma ray can pass through any material; it can cause severe damage to the cells of human beings. Hence, an increase in the representative gamma index greater than the universal standard of unity may result in radiation risk leading to the deformation of human cells thereby causing cancer. This index is used to correlate the annual dose rate due to the excess external gamma radiation caused by superficial materials and acts as a screening tool for identifying materials that might become health concerns when used as construction materials [18]. In this study, the gamma index (I<sub>γ</sub>) was calculated as proposed by the European Commission [11, 19].

$$RLI = \frac{1}{150 A_{Ra}} + \frac{1}{100 A_{Th}} + \frac{1}{1500 A_K} \text{ ----- (5)}$$

Values of I<sub>γr</sub> ≤ 1 corresponds to an annual effective dose of less than or equal to 1mSv, while I<sub>γr</sub> ≤ 0.5 corresponds to annual effective dose less or equal to 0.3 [20]. The calculated values of the representative level index vary from 0.311 (CNK) to 2.182(CVM) with mean value of 0.702 (Table 2). The representative level index (I<sub>γr</sub>) must be less than unity in order to keep the radiation hazard insignificant [11]. The mean I<sub>γr</sub> value (0.70) in the study area is below the recommend value indicating that the

sediments do not pose any hazard. Fig.5 shows the variation of Representative level index (I<sub>γr</sub>) at different sampling locations.

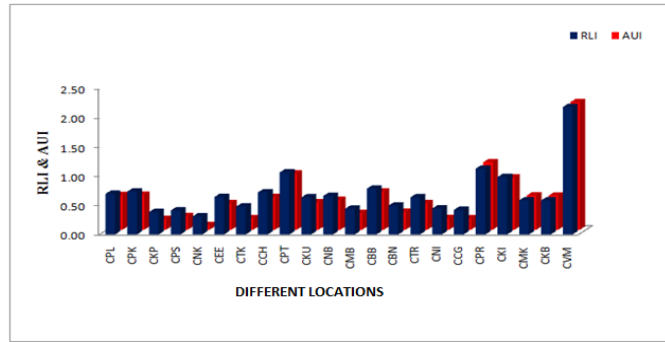


**Fig.5.** Locations Vs RLI & AUI.

### 3.2.6 Activity Utilization Index (AUI)

In order to facilitate the calculation of dose rates in air from different combinations of the three radionuclides in sediments and by applying the appropriate conversion factors, an activity utilization index (AUI) is constructed for the usage of construction materials that is given by the following formula [11, 21].

$$AUI = \left(\frac{A_U}{50 \text{ Bq/kg}}\right) f_U + \left(\frac{A_{Th}}{50 \text{ Bq/kg}}\right) f_{Th} + \left(\frac{A_K}{500 \text{ Bq/kg}}\right) f_K \text{ ----- (6)}$$

Where A<sub>U</sub>, A<sub>Th</sub> and A<sub>K</sub> are activity concentrations (in Bq kg<sup>-1</sup>) of <sup>238</sup>U, <sup>232</sup>Th and <sup>40</sup>K and f<sub>U</sub>, f<sub>Th</sub>, and f<sub>K</sub> are the fractional contributions to the total dose rate in air due to gamma radiation from the actual concentrations of these radionuclides. A<sub>U</sub>, A<sub>Th</sub> and A<sub>K</sub> are referred to be 50, 50 and 500 Bq kg<sup>-1</sup> respectively [22].

The activity utilization index of the sediment samples are calculated using the above formula. The calculated values (Table 2) vary from 0.080 (CNK) to 2.357 (CVM) with an average of 0.552. This value shows that AUI is less than 0.3 mSv y<sup>-1</sup> for all locations, which corresponds to an annual effective dose < 0.3 mSv y<sup>-1</sup> [23, 24]. This indicates that these sediments can be safely used for construction purposes. Fig. 5 shows variation of activity utilization index (AUI) with different locations.

### 3.3 Radiation Hazard Indices

Different known radiation health hazard indices analysis is been use in radiation studies to arrive at a better and safer conclusion on the health status of a radiated or irradiated person and environment in recent studies [25-29]. To assess the radiation hazards associated with the studied samples, the following indices have been defined.

#### 3.3.1 Internal Hazard Index (H<sub>int</sub>)

In addition to the external hazard, radon and its short-lived products are also hazardous to the respiratory organs. Internal exposure to radon and its daughter products are

very hazardous and can lead to respiratory diseases like asthma and cancer. The internal exposure to radon and its daughter products is quantified by the internal hazard index ( $H_{int}$ ) which is given by the equation. This hazard can be quantified by the internal hazard index ( $H_{int}$ ) [9, 11, 24, 30].

$$H_{int} = \frac{A_U}{185 \text{ Bq/kg}} + \frac{A_{Th}}{259 \text{ Bq/kg}} + \frac{A_K}{4810 \text{ Bq/kg}} \quad \text{--- (7)}$$

The average value of  $H_{int}$  has been determined to be 0.279 (Table 2) is less than permissible limit. The above results indicate that the internal hazard is below the critical value and has no significant radiation hazards associated with the sediments and hence the coastal sediments are unlikely to pose radiological health risk to the people living in nearby areas along the East coast of Tamilnadu, India. Fig. 6 shows variation of  $H_{int}$  with different locations.

### 3.3.2 External hazard index ( $H_{ex}$ )

The External Hazard Index is an evaluation of the hazard of the natural gamma radiation [31]. This index is used to assess the radiological suitability of a material. The external hazard index ( $H_{ex}$ ) represents the external radiation exposure associated with gamma radiation from radionuclides of concern. This index can be evaluated using the following equation.

$$H_{ext} = \frac{A_U}{370 \text{ Bq/Kg}} + \frac{A_{Th}}{259 \text{ Bq/Kg}} + \frac{A_K}{4810 \text{ Bq/Kg}} \quad \text{--- (8)}$$

The calculated value of the External Hazard Index for the studied samples is presented in Table 2. The  $H_{ex}$  values ranged from 0.100 (CNK) to 0.825 (CVM) with an average value of 0.251. The value of  $H_{ex}$  must be lower than unity in order to keep the radiation hazard insignificant. The obtained values of  $H_{ex}$  indicates that sediments may not do harm to workers and peasants in this region. Further, the mean value of the results showed there were no elevated radiological health hazards to the people living in nearby terrestrial areas of the sampling sites and the people who handle the marine sediments for utilizing them in building constructions is safe. The higher value of  $H_{ex}$  in Vadanemmeli may be due to the dynamic movement of finer sediments from coastal regions, local industrial activities and movement of fishing/commercial vessels in this region. Fig. 6 shows variation of  $H_{ex}$  with different locations.

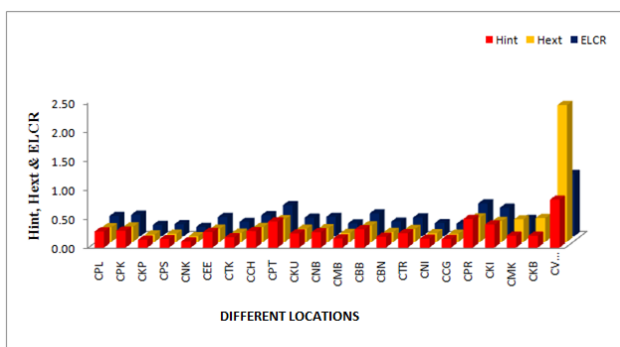


**Fig. 6.** Locations Vs Internal, External Hazard Indices & Excess Lifetime cancer Risk

### 3.3.3 Excess Lifetime Cancer Risk (ELCR)

This deals with the probability of developing cancer over a lifetime at a given exposure level. It is presented as a value representing the number of cancers expected in a given number of people on exposure to a carcinogen at a given dose. It is worth noting that an increase in the ELCR causes a proportionate increase in the rate at which an individual can get cancer of the breast, prostate or even blood. Potential carcinogenic effects are characterized by estimating the probability of cancer incidence in a population of individuals for a specific lifetime from projected intake, exposures and chemical-specific dose-response data (i.e., slope factors). The additional or extra risk of developing cancer due to exposure to a toxic substance incurred over the lifetime of an individual [17]. The Excess lifetime cancer risk (ELCR) is calculated using below equation [32].

$$ELCR = AEDE \times DL \times RF \quad \text{--- (9)}$$

where AEDE, DL and RF are the total Annual Effective Dose Equivalent, duration of life (70 years) and risk factor ( $Sv^{-1}$ ), i.e. fatal cancer risk per sievert, respectively. For stochastic effects, ICRP 60 uses values of 0.05 for the public [32].

From Table 2, the calculated ELCR values ranged from  $0.161 \times 10^{-3}$  (CNK) to  $1.071 \times 10^{-3}$  (CVM) with an average of  $0.353 \times 10^{-3}$ , which is slightly higher than the worldwide recommended value of  $0.29 \times 10^{-3}$  [1]. ELCR Values in all the locations are slightly higher than the world average recommended limit except Kattupalli (CKP)  $0.195 \times 10^{-3}$ , Power Station (CPS)  $0.208 \times 10^{-3}$ , Nettukuppam (CNK)  $0.161 \times 10^{-3}$ , Tiruchinnakuppam (CTK)  $0.248 \times 10^{-3}$ , Marina Beach (CMB)  $0.221 \times 10^{-3}$ , Besant Nagar (CBN)  $0.252 \times 10^{-3}$ , Nellankarai (CNI)  $0.226 \times 10^{-3}$ , Chennai Golden Beach (CCG)  $0.215 \times 10^{-3}$ , may be due to the higher activity concentration of  $^{232}Th$  which reflects enhancing value of ELCR. Fig. 6 shows the locations and excess lifetime cancer (ELCR) values.

## 4 Statistical Analyses

The multivariate statistical method can also help to simplify and organize large data sets to indicate natural associations between samples and/or variables. Various statistical analyses have been carried out for the data obtained from radioactivity analysis of sediments using software SPSS16.0 by Statistical Graphics. These methods were as follows:

- Basic statistics
- Principal component analysis
- Correlation analysis
- Cluster analysis

### 4.1 Basic Statistics of Natural Radionuclides

Table 4 shows the basics statistics such as minimum, maximum, mean, standard deviation, variance, skewness and kurtosis of natural radionuclides from Pulicat lake to

Vadanemmel. In the present study, standard deviation of  $^{238}\text{U}$ ,  $^{232}\text{Th}$  and  $^{40}\text{K}$  are smaller than their mean value. This shows that concentration of uranium and thorium in sediment samples has high degree of uniformity in their distribution [11]. Skewness refers to the asymmetry or lack of symmetry in the shape of a frequency distribution. When a distribution is not symmetrical it is called a skewed distribution. Skewed distribution could either be positively or negatively skewed [11]. In the present study, the skewness of activity concentrations of  $^{238}\text{U}$ ,  $^{232}\text{Th}$  and  $^{40}\text{K}$  radionuclides are positive, which shows that their distributions are asymmetric. Kurtosis is a measure of peakedness. It is also a function of internal sorting or distribution. Depending upon the peakedness, it is named as mesokurtic, leptokurtic and platykurtic. If the value of kurtosis is zero, it is known as normal curve or mesokurtic. When the kurtosis value is positive, the curve is more peaked than the normal curve i.e., leptokurtic whereas the negative value of kurtosis indicates less peaked than the normal curve i.e., platykurtic [11, 33]. In the present study, the kurtosis value of activity concentrations of  $^{238}\text{U}$ ,  $^{232}\text{Th}$  and  $^{40}\text{K}$  is positive and it indicates that the curve is more peaked than the normal curve i.e., leptokurtic. The frequency distribution of  $^{238}\text{U}$ ,  $^{232}\text{Th}$  and  $^{40}\text{K}$  are shown in Fig 7-9. The normal bell shaped curve was obtained for  $^{40}\text{K}$ . This indicates that the  $^{40}\text{K}$  does not involve in the hazardous. The multimodality structure of  $^{238}\text{U}$  and  $^{232}\text{Th}$  indicates that the radiological hazards are controlled by  $^{238}\text{U}$  and  $^{232}\text{Th}$  only.

#### 4.2 Principal Component Analysis (PCA) Among Radionuclides and Radiological Parameters

PCA is a multivariate statistical technique that is used to reduce data and decipher patterns within large sets of data [34]. Data reduction is performed by transforming data to a new set of variables (principal components) that are derived from linear combinations of the original variables and classified in such a way that the first principal components (typically two or three) are responsible for most of the variation in the original dataset [35-37]. The number of components to keep is based on the Kaiser criterion, for which only the components with eigen values greater than 1 are retained. As a result, all components that contain a greater variance than the original standardized variables are kept [38].

**Table 4.** Summary of basic statistics

Variables	$^{238}\text{U}$	$^{232}\text{Th}$	$^{40}\text{K}$
Minimum	2.21	2.11	330.91
Maximum	31.03	168.4	540.02
Mean	10.14	35.01	425.82
Std. Deviation	7.85	34.89	47.66
Variance	61.66	1218	2272
Skewness	1.295	2.885	0.044
Kurtosis	1.519	10.312	0.756
Frequency distribution	Log-Normal	Log-Normal	Normal

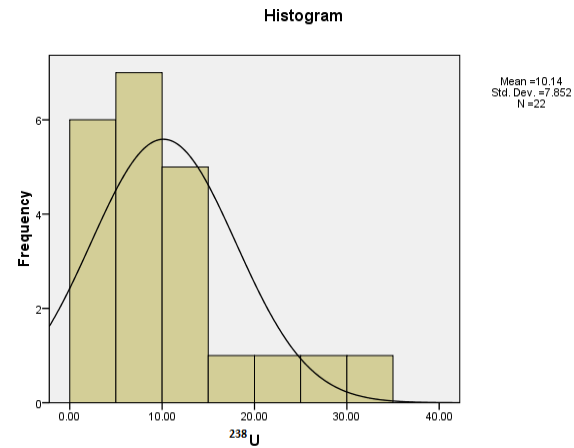


**Fig. 7.** Frequency distribution of  $^{238}\text{U}$ .

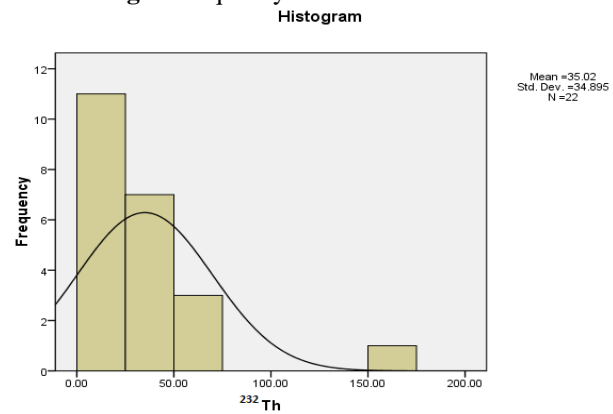


**Fig. 8.** Frequency distribution of  $^{232}\text{Th}$ .

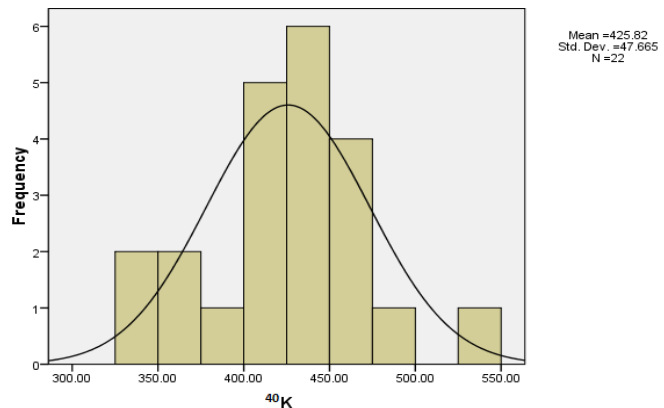


**Fig. 9.** Frequency distribution of  $^{40}\text{K}$ .

Using this technique, a system of components is obtained through the transformation of radio elements and their ratios. These new components are constrained to reproduce as much as possible the total variance of the original data. To maximize the variance of the principal components, the Varimax normalized rotation was applied. Obtained importance principal components such as component 1 and 2 are given in Table 5 and shown in Fig. 10.



The principal component 1 extracted due to high positive loading of  $^{238}\text{U}$  and  $^{232}\text{Th}$  associated with all radiological parameters with explained variance of 90.01%. This indicated that the total level of natural radioactivity in the study area due to concentration of uranium and thorium only. Similarly component 2 due to low positive loadings of  $^{238}\text{U}$  and  $^{232}\text{Th}$  with  $^{40}\text{K}$  explained variance of 8.45% but concentration of potassium not controls the levels of radioactivity. According to [11, 17] If the total variance is greater than 70%, the fitted principal components to the data were good. In the present study the total explained variance is 98.46% to the radioactive data's.

**Table 5:** Rotated factor loadings of variables

Variables	Component-1	Component-2
$^{238}\text{U}$	0.906	0.043
$^{232}\text{Th}$	0.995	-0.081
$^{40}\text{K}$	0.003	1
Req	1	0
DR	1	0.023
HR	1	0.024
AUI	0.998	-0.056
AGDE	1	0.025
Hint	0.998	0.004
Hext	1	0
ELCR	1	0.022
<b>% of variance explained</b>	<b>90.01%</b>	<b>8.45%</b>

**Fig. 10.** Graphical representation of component 1 & 2.

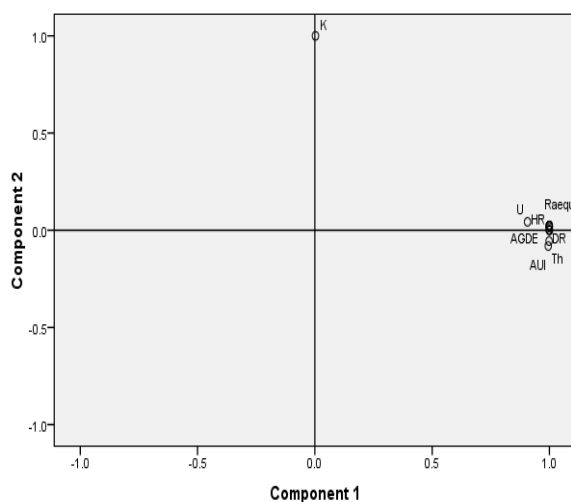
### 4.3 Pearson Correlations among Radionuclides and Derived Radiological Parameters

The linear relationship of radionuclides and associated radiological parameters was determined using Pearson's correlation coefficient analysis and are presented in Table 6. The correlation of  $^{238}\text{U}$  with  $^{232}\text{Th}$  showed a fairly high degree of positive correlation coefficient of  $r > 0.75$ , suggesting that the sediments are mostly influenced and controlled by similar origin of sources [17]. A very low degree of correlation was seen of  $^{238}\text{U}$ ,  $^{232}\text{Th}$  and  $^{40}\text{K}$ , it suggesting that  $^{238}\text{U}$ ,  $^{232}\text{Th}$  and  $^{40}\text{K}$  were of dissimilar origin in sediments.  $^{238}\text{U}$  and  $^{232}\text{Th}$  showed a high degree of positive correlation with all radiological hazard parameters except  $^{40}\text{K}$ . This indicated that radiological hazards were associated with uranium and thorium concentration and potassium is not influence of radiological hazards. Finally the Pearson Correlation Analysis is in good agreement with Principal Component Analysis.

### 4.4 Cluster Analysis (CA) among Radionuclides and Hazard Parameters (Dendrogram)

Cluster analysis is one of multivariate techniques used to identify and classify groups with similar characters in a new group of observations. Each observation in a cluster is most like others in the same cluster. Cluster analysis was carried out through two axes; the first axis was to identify distance. The other axis was to identify similar characteristics among radiological parameters. To confirm the existing correlation between the variables, cluster analysis (CA) is carried out. In CA, single linkage method along with correlation coefficient distance is applied.

Component Plot in Rotated Space



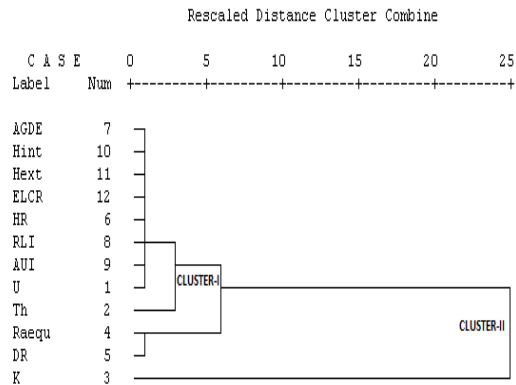
The dendrogram visually displays the order in which parameters or variables combine to form clusters with similar properties. The most similar objects are first grouped, and these initial groups are merged according to their similarities. Similarity is a measure of distance between clusters relative to the largest distance between any two individual variables. One hundred percent similarity means the clusters were zero distance apart in their sample measurements, while the similarity of zero percent means the cluster areas are as disparate as the least similar region [21]. The derived dendrogram is shown in Fig.11.

In this dendrogram, all 12 parameters are grouped into two statistically significant clusters. All the clusters are formed on the basis of existing similarities. Cluster I consists of natural radionuclides ( $^{238}\text{U}$  and  $^{232}\text{Th}$ ) and all important radiological parameters with high similarity. This shows that the total level of radioactivity in sediment mainly depends on the corresponding  $^{238}\text{U}$  and  $^{232}\text{Th}$  concentrations.

**Table 6: Pearson correlations between radionuclides and associated radiological hazards**

Variables	<sup>238</sup> U	<sup>232</sup> Th	<sup>40</sup> K	Ra(eq)	D <sub>R</sub>	HR	AGDE	RLI	AUI	H <sub>int</sub>	H <sub>ext</sub>	ELCR
<sup>238</sup> U	1											
<sup>232</sup> Th	0.873	1										
<sup>40</sup> K	0.044	-0.078	1									
Ra(eq)	0.909	0.995	0.002	1								
D <sub>R</sub>	0.914	0.992	0.025	1	1							
HR	0.913	0.992	0.027	1	1	1						
AGDE	0.911	0.992	0.028	1	1	1	1					
RLI	0.908	0.993	0.017	1	1	1	1	1				
AUI	0.907	0.997	-0.053	0.998	0.997	0.997	0.997	0.997	1			
H <sub>int</sub>	0.929	0.99	0.007	0.999	0.999	0.999	0.999	0.999	0.997	1		
H <sub>ext</sub>	0.908	0.995	0.002	1	1	1	1	1	0.998	0.999	1	
ELCR	0.914	0.992	0.025	1	1	1	1	1	0.997	0.999	1	1

Dendrogram using Average Linkage (Between Groups)

**Fig. 11.** Shows the clustering of radioactive variables

Cluster II consists of <sup>40</sup>K only, suggesting that concentration of potassium in sediments do not contribute to the radiation hazard in the sediment sampling locations. The result of the cluster analysis is in good agreement and matches well with Pearson correlation analysis and principal component analysis.

## 5 Conclusion

In this study, the gamma radiation has been measured to determine natural radioactivity of <sup>238</sup>U, <sup>232</sup>Th and <sup>40</sup>K in collected sediment samples from Pulicat lake to Vadanemeli of Chennai coast, Tamilnadu. The average activity of <sup>232</sup>Th is slightly higher compared with the world average value. All the measured radiological parameters are less than the permissible limit except some locations of Panaiyur(CPR), Kanathursunami (CKI) and Vadanemeli (CVM). This may be due to the presence of heavy minerals and rich black sand in these locations. Moreover, it is also due to the recent development of major industries, shipping

and harbor activities. The multivariate statistical analysis gives good agreement with the radioactive variables.

## Acknowledgments

One of the authors (R. Ravisankar) wishes to express his high gratitude to **Dr. B. Venkatraman**, Director, Health, Safety and Environmental Group (HSEG), Indira Gandhi Centre for Atomic Research (IGCAR), Kalpakkam, Tamil Nadu, India, for giving permission to use the nuclear counting facility in Radiological Safety Division (RSD). Our special thanks to **Dr. M. T. Jose**, Head, RSD, IGCAR, for his keen help, constant encouragements in gamma ray spectroscopic measurements and also **Mr. R. Mathiarasu**, Scientific Officer, RSD, IGCAR, for his technical help in counting the samples.

## References

- [1] UNSCEAR, United Nations Scientific Committee on the Effects of Atomic Radiation. Sources, Effects and Risks of Ionizing Radiation. Report to the General Assembly with annex B, United Nations, NewYork. 2000.
- [2] UNSCEAR, United Nations Scientific Committee on the Effects of Atomic Radiation. Sources, Effects and Risks of Ionizing Radiation. United Nations, NewYork. 1988.
- [3] Mohsen B. Challan and A. El-Taher Analytical approach for radioactivity correlation of disc sources with HPGe detector efficiency Journal of Applied Radiation and Isotopes. **85**, 23-27(2014).
- [4] Alatise OO, Babalola IA and Olowofela JA. Distribution of some natural gamma emitting radionuclides in the soils of the coastal areas of Nigeria. J. Environ. Radioact., **99**, 1746-1749(2008).
- [5] Tari M, Zarandi SAM, Mohammadi K and Zare MR. The measurement of gamma-emitting radionuclides in

- beach sand cores of coastal regions of Ramsar, Iran using HPGe detectors. *Mar. Pollut. Bull.* **74**, 425-434(2013).
- [6] Mora Sde, Sheikholeslami MR, Wyse E, Azemard S and Cassi R. An assessment of metal contamination in coastal sediments of the Caspian Sea. *Mar. Pollut. Bull.*, **48**, 61-77(2004).
- [7] H. A Madkour and A El-Taher Environmental studies and Radio-Ecological Impacts of Anthropogenic areas: Shallow Marine Sediments Red Sea, Egypt. *Journal of Isotopes in Environment and Health Studies.*, **50**, 120 - 133(2014).
- [8] Alfonso JA, Perez K, Palacios D, Handt H, LaBrecque JJ, Mora A and Vasquez Y. Distribution and environmental impact of radionuclides in marine sediments along the Venezuelan coast. *Journal of Radioanalytical and Nuclear Chemistry.*, **300**, 219–224(2014).
- [9] Beretka J and Matthew PJ. Natural radioactivity of Australian building materials. *Industrial wastes and by-products. Health Phys.*, **48**, 87–95(1985).
- [10] Amekudzie A, Emi-Reynolds G, Faanu A, Darko EO, Awudu AR, Adukpon O, Quaye LAN, Kporozro R, Agyemang B and Ibrahim A. Natural Radioactivity Concentrations and Dose Assessment in Shore Sediments along the Coast of Greater Accra, Ghana. *W. Appl. Sci. Jour.*, **13**, 2338-2343(2011).
- [11] Ravisankar R, Chandramohan J, Chandrasekaran A, Prince Prakash Jebakumar J, Vijayalakshmi I, Vijayagopal P and Venkatraman B. Assessments of radioactivity concentration of natural radionuclides and radiological hazard indices in sediment samples from the East coast of Tamilnadu, India with statistical approach, *Marine Pollution Bulletin.*, **97**, 419–430(2015).
- [12] Atef El-Taher, Hesham M.H. Zakaly, Reda Elsaman Environmental implications and spatial distribution of natural radionuclides and heavy metals in sediments from four harbours in the Egyptian Red Sea coast. *Applied Radiation and Isotopes.*, **131**, 13–22(2018).
- [13] Kurnaz A, Kucukomeroglu B, Keser R, Okumusoglu NT, Korkmaz F, Karahan G and Cevik U. Determination of radioactivity levels and hazards of soil and sediment samples in Firtina Valley (Rize, Turkey). *Applied Radiation and Isotopes.*, **65**, 1281–1289(2007).
- [14] ICRP (International Commission on Radiological Protection). ICRP Publication 65, *Annals of the ICRP*. Pergamon Press, Oxford., **23**(2), 1993
- [15] UNSCEAR, United Nations Scientific Committee on the Effects of Atomic Radiation. *Sources, Effects and Risks of Ionizing Radiation*. United Nations, New York. 1993.
- [16] A. El-Taher and H. A. Madkour Texture and Environmental Radioactivity Measurements of Safaga Sand dunes, Red Sea, Egypt *Indian journal of Geo-Marine Science.*, **42**(1), 35-41(2013).
- [17] Ravisankar R, Sivakumar S, Chandrasekaran A, Prince Prakash Jebakumar J, Vijayalakshmi I, Vijayagopal P and Venkatraman B. Spatial distribution of gamma radioactivity levels and radiological hazard indices in the East coastal sediments of Tamilnadu, India with statistical approach, *Radiation Physics and Chemistry.*, **103**, 89-98(2014).
- [18] Jibiri NN and Okeyode IC. Evaluation of radiological hazards in the sediments of Ogun River, South-Western Nigeria. *Radiation Physics and Chemistry.*, **81**, 103–112(2012).
- [19] European Commission (EC). *Radiation protection 112. Radiological Protection Principles Concerning the Natural Radioactivity of Building Materials*, Directorate- General Environment. Nuclear Safety and Civil Protection. 1999.
- [20] Turham S and Gunduz L. Determination of specific activity of  $^{226}\text{Ra}$ ,  $^{232}\text{Th}$  and  $^{40}\text{K}$  for assessment of radiation hazards from Turkish plumice samples. *Journal of environmental radiation*. doi: 10.1016/j.jenvrad.2007.08.002. 2007.
- [21] Ramasamy V, Suresh G, Meenakshisundaram V and Ponnusamy V. Horizontal and vertical characterization of radionuclides and minerals in river sediments, *Appl Radiat Isot.*, **69**, 184-95(2011).
- [22] NEA-OECD. *Exposure to Radiation from Natural Radioactivity in Building Materials*. Report by NEA Group of Experts of the Nuclear Energy Agency. OECD, Paris, France. 1979.
- [23] Hashem A. Madkour , Mohamed Anwar K abdelhalim , Kwasi A. Obirikorang , Ahmed W. Mohamed and Abu El-Hagag N. Ahmed and A. El-Taher Texture and Geochemistry of Surface Sediments in Coastal Lagoons from Red Sea Coast and their Environmental Implications. *Journal of Environmental Biology.*, **36**, 5(2015).
- [24] Chandrasekaran A, Ravisankar R, Senthilkumar G, Thillaiavelavan K, Dhinkaran B, Vijayagopal P, Bramha SN and Venkatraman B. Spatial distribution and lifetime cancer risk due to gamma radioactivity in Yelagiri Hills, Tamilnadu, India. *Egyptian Journal of Basic and Applied Sciences.*, **1**, 38-48(2014).
- [25] Avwiri GO, Osimobi JO and Agbalagba EO. Evaluation of Radiation Hazard Indices and Excess Lifetime Cancer Risk Due to Natural Radioactivity in soil profile of Udi and Ezeagu Local Government Areas of Enugu State, Nigeria. *Journal of Environmental and Earth Sciences*, **1**(1), 1-10(2012).
- [26] Orgun Y, Altinsoy N, Sahin SY, Gungor Y, Gultekin AH, Karaham G and Karaak Z. Natural and anthropogenic radionuclide in rocks and beach sands from Ezine region, Western Anatolia, Turkey. *Applied Radiation and Isotopes.*, **65**, 739- 747(2007).
- [27] A.El-Taher and M.A.M.Uosif The Assessment of the Radiation Hazard Indices due to Uranium and Thorium in Some Egyptian Environmental Matrices. *Journal of Physics. D: Applied Physics.*, **39**, 6-4521(2006).

- [28] S. Makhluif and A. El-Taher Radiological Significance of Egyptian Limestone and Alabaster used for Construction of Dwellings. *Indian Journal of pure and applied physics* ., **49**, 157-161(2011).
- [29] M.A.M.Uosif and A. El-Taher Comparison of Total Experimental and Theoretical Absolute gamma ray Detection Efficiencies of a Cylindrical NaI (Ti) Crystal. *Arab Journal of Nuclear Science and Applications*., **38**, 357-365(2005).
- [30] Hashem Abbas Madkour, A. El-Taher, Abu El-Hagag N. Ahmed, Ahmed W. Mohamed and Taha M. El-Erian Contamination of coastal sediments in El-Hamrawein Harbour, Red Sea Egypt. *Journal of Environmental Science and Technology*, **5(4)** , 2012.
- [31] S. Makhluif and A. El-Taher Radiological Significance of Egyptian Limestone and Alabaster used for Construction of Dwellings. *Indian Journal of pure and applied physics*.,**49**, 157-161(2011).
- [32] Taskin H, Karavus M, Ay P, Topuzoglu A, Hindiroglu and Karajan G. Radionuclide concentrations in soil and lifetime cancer risk due to the gamma radioactivity in Kirklareli, Turkey. *J. Environ. Radioact.*,**100**, 49–53(2009).
- [33] Gupta SP. *Statistical Methods*. Sultan Chand & Sons, Educational Publishers, New Delhi. 2001
- [34] Chen K, Jiao JJ, Huang J and Huang R. Multivariate statistical evaluation of trace elements in groundwater in a coastal area in Shenzhen, China. *Environ. Pollut.* **147**, 771–780(2007).
- [35] Everitt BS and Hothorn T. *An Introduction to Applied Multivariate Analysis with R*. Springer, New York. ISBN 978-1-4419-9649-7, 2011.
- [36] Matiatos I, Alexopoulos A and Godelitsas A. Multivariate statistical analysis of the hydrogeochemical and isotopic composition of the groundwater resources in northeastern Peloponnesus (Greece). *Sci. Total Environ.***476–477**:577–590, 2014.
- [37] Ogwueleka TC. Use of multivariate statistical techniques for the evaluation of temporal and spatial variations in water quality of the Kaduna River, Nigeria. *Environ. Monit. Assess.***187**:137, 2015.
- [38] Davis JC. John Wiley and Sons Inc., New York, USA. *Statistics and Data Analysis in Geology*. 1986.